

Compatibility of polyvinyl alcohol and poly(methyl vinyl ether-*co*-maleic acid) blends estimated by molecular dynamics

F.S. Moolman^{a,*}, M. Meunier^b, P.W. Labuschagne^a, P.-A. Truter^a

^aCenter for Polymer Technology, CSIR, P.O. Box 395, Pretoria 0001, South Africa

^bAccelrys Ltd, 334 Cambridge Science Park, Cambridge CB4 0WN, UK

Received 2 February 2005; received in revised form 29 March 2005; accepted 29 March 2005

Available online 15 June 2005

Abstract

The CSIR has developed a novel oxygen barrier technology for plastics packaging based on interpolymer complex formation between PVOH (polyvinyl alcohol) and PMVE-MA (poly(methyl vinyl ether-*co*-maleic acid)). As interpolymer complexation interactions are strongly dependent on stoichiometric ratios, the estimation of the optimum blend ratio is an important component of blend design.

This study used molecular dynamics modelling to predict the ratio of optimum interaction for PVOH:PMVE-MA blends. Amorphous cells were constructed containing blends of short-chain repeat units of PVOH and PMVE-MA. The oligomers were equilibrated using both NVT and NPT dynamics and the cohesive energy densities (CED's) of the models were computed. From the CED's, energies of mixing and Flory–Huggins Chi Parameter (χ) values were estimated.

The χ -values were negative for all blends, indicating favorable interaction between the two polymers. The minimum χ -values were found around 0.6–0.7 mass fraction of PMVE-MA, which agrees well with experimental viscosity results (this work), which indicated optimum interaction around 0.7 mass fraction PMVE-MA. These results confirm that molecular dynamics can be used as a tool for investigating interpolymer complexation phenomena.

© 2005 Elsevier Ltd. All rights reserved.

Keywords: Interpolymer complexation; Hydrogen bonding; Molecular dynamics

1. Introduction

PET (polyethylene terephthalate) is a polymer extensively utilized in plastics packaging applications, especially for carbonated soft drinks packaging, and in recent years has been steadily replacing other packaging materials (e.g. glass, aluminum cans, polyethylene) in a range of applications. The main reason for the popularity of PET for carbonated soft drinks packaging is the favorable properties, namely low CO₂ permeability (permeability coefficient $P_{\text{CO}_2} = 1.18 \times 10^{-14} \text{ cm}^3 \text{ (STP) cm/cm}^2 \text{ s Pa}$ [1]), processability, transparency and the fact that it is shatterproof. While its oxygen permeability is lower than most other thermoplastics [1], it is still not low enough to permit packaging of oxygen-sensitive products such as

milk, fruit juice and beer in PET with sufficient shelf life. Consequently, a number of technologies have recently appeared on the market attempting to remedy this. These include multilayers, alternative polymers (e.g. PEN or polyethylene naphthalate), inside coatings of e.g. SiO_x and outside coatings such as a spray-coated epoxy-amine [2].

The CSIR in South Africa is developing a proprietary barrier technology for plastics packaging applications that can be applied to PET and other thermoplastics such as PP (polypropylene) [3]. This technology consists of an oxygen barrier layer and a protective overcoat as a moisture barrier. The oxygen barrier layer utilizes interpolymer complexation to improve the barrier properties.

Interpolymer complexation is the favorable (non-covalent) interaction between two complementary polymers through e.g. electrostatic interactions, hydrophobic interactions, hydrogen bonding or Van der Waals interactions [4, 5]. The CSIR's technology uses a blend of PVOH (polyvinyl alcohol) and PMVE-MA (polymethyl vinyl ether-*co*-maleic acid) (Fig. 1), which forms an interpolymer complex through hydrogen bonding between the alcohol groups of

* Corresponding author. Tel.: +27 12 841 4212; fax: +27 12 841 3553.
E-mail address: smoolman@csir.co.za (F.S. Moolman).

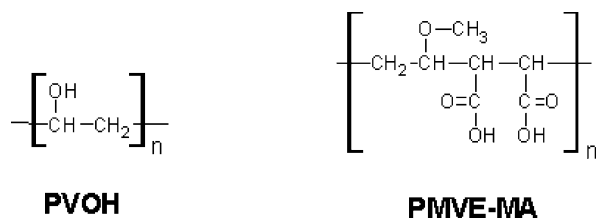


Fig. 1. Repeat units of PVOH and PMVE-MA.

the PVOH and the carboxylic acid and ether groups of the PMVE-MA.

With interpolymer complexes, the extent of interaction is dependent on the stoichiometric ratio between the two components in the blend, and in most cases, a region of maximum interaction can be observed. One of the simplest ways of determining the optimum stoichiometric ratio for water-soluble polymers is through measurement of blend viscosities.

In the past decade, molecular modelling has been successfully employed to help solve critical industrial problems [6,7]. In the case of polymer science, many physico-chemical properties have been accurately computed using modelling techniques [8] (e.g. permeability [9], compatibility [10], etc.). Many different algorithms can be employed to compute those properties—amongst them molecular dynamics have been particularly popular as it allows the computation of time dependent properties. However, many other methods have been used, e.g. group additive method [11] and methods based on quantum mechanics for the calculation of e.g. electronic properties— for a review, please see Refs. [12,13].

In this study, molecular dynamics modelling was used to predict optimum blend ratios (in terms of maximum interaction) for blends of PVOH and PMVE-MA and the results were compared with experimental work. Such in silico experiments significantly contribute towards reducing costly ‘trial-and-error’ experiments and, if accurate enough to predict the optimum blend ratios for a wide range of materials, could routinely be employed for screening of polymer blends for complex formation.

2. Materials and methods

2.1. Materials

PVOH is normally manufactured through the hydrolysis of polyvinyl acetate. The hydrolysis reaction is never 100% complete and thus a range of polyvinyl acetates with different degrees of hydrolysis is available on the market. In this set of experiments, Celvol 107 (Celanese Chemicals, 98.4% hydrolysed, degree of polymerization 350–650) was used. The PMVE-MA used was Gantrez S97 (ISP, approx. M_w 1,500,000 g/mol).

2.2. Experimental methods

For the viscosity experiments, 10% solutions of PVOH and PMVE-MA were prepared by slowly adding 100 g of the polymer to 900 g of hot water (80 °C) in a sealable glass container while stirring, and then leaving the sealed container in a preheated oven for 16 h (95 °C for PVOH and 60 °C for PMVE-MA). The solutions were subsequently stirred with a magnetic stirrer until completely dissolved and cooled down before use. The blends were made up so that the total polymer content was always a mass fraction of 10%. A brookfield digital viscometer (Model DV-1) with spindle RV-4 (rotating at 100 rpm) was used to measure the solution viscosities. pH was measured using a pH209 pH-meter from Hanna instruments.

The density of the PMVE-MA was determined experimentally through measurement of volume replacement and mass. Briefly, a film was cast from a 10% solution in water into a Petri dish. The solution was dried overnight in a vacuum oven at 60 °C. The film was then weighed before suspending it in isooctane (Merck, 99% pure), which is a non-solvent for Gantrez S97, and the increase in volume was measured.

The solubility range for Gantrez S97 was determined using ASTM D3132-84 (1996): standard test method for solubility range of resins and polymers.

2.3. Computational details

For the molecular dynamics simulations, the codes discover and amorphous_cell of the materials studio[®] suite of software were used [14]. Different configurations of the polymer chains have been generated and placed in a cubic box using the amorphous_cell code based on the ‘self-avoiding’ random-walk method of Theodorou and Suter [15] and on the Meirovitch scanning method [16]. For indication of results trends, simple polynomials were fitted to the data using microsoft excel’s built in linear regression functions.

The basic steps for generating the periodic amorphous cells containing blends of PVOH and PMVE-MA were as follows:

1. Generation of short-chain polymers with 10 repeat units each (isotactic, head-to-tail).
2. Minimization of the energy of the model polymers through 5000-step energy minimization on each (using the COMPASS force field [14]), to remove high-energy areas (e.g. overlapping atoms).
3. Build 20 periodic amorphous cells of each of the 11 different blend ratios (Table 1), with a target density of 1.1 g/cm³, at a temperature of 300 K.
4. Run a ‘basic refine’ protocol (consisting of a NVT molecular dynamics run of 4000 fs using a 0.25 fs timestep, at 300 K)—bonds were kept fixed during the runs.

Table 1
Polymer ratio and mass fraction of the systems studied

Approximate mass ratio (PVOH:PMVE-MA)	1:0	9:1	8:2	7:3	6:4	5:5	4:6	3:7	2:8	1:9	0:1
PVOH (no. of molecules)	24	30	19	19	17	12	10	8	6	3	0
PMVE-MA (no. of molecules)	0	1	1	2	3	3	4	5	6	7	6
Cell length at equilibrated density (Å)	25.1	28.0	24.4	25.6	26.0	24.2	24.7	25.3	25.7	25.9	23.7
Mass fraction PMVE-MA	0	0.12	0.17	0.29	0.41	0.50	0.61	0.71	0.80	0.90	1

- The five lowest energy cells from each of the 11 blend ratios from step 4 were selected. Low or zero density areas were removed through a temperature cycle run (NPT dynamics)—11 stages of 5000 fs (temperatures from 300 to 700 K) and 11 stages from 700 to 300 K.
- Then, NPT dynamics were employed until the density converged (about 250–350 ps), using the velocity scaling thermostat and Andersen barostat, $P=0.0001$ GPa, 300 K.
- The total energy was equilibrated through a NVT dynamics run of 30 ps using the Berendsen thermostat at 300 K.
- For the production run, NVT dynamics of 100 ps were performed.

Both polymers had 10 repeat units, with $M_{\text{PVOH}}=442.54$ g/mol and $M_{\text{PMVE-MA}}=1743.53$ g/mol. Eleven blend compositions were modelled as shown in Table 1. For each of the 11 blend compositions, three sets of 20 cells each were generated, and the five lowest energy cells for each of the three sets were then selected, giving 15 cells per blend composition.

3. Results

3.1. Equilibration

Fig. 2 shows the density of a selected number of runs (cells 11–15) as function of time during the NPT density equilibration. It can be clearly seen that density has been sufficiently equilibrated in this step. For these five runs, densities (with standard deviations in brackets to indicate extent of variability between runs) were as follows: PVOH 1.118 (± 0.009) g/cm³; PMVE-MA 1.318 (± 0.023) g/cm³ and PVOH:PMVE-MA 50:50 1.232 (± 0.016) g/cm³.

The potential and kinetic energies of all the cells during NVT dynamics were plotted as a function of time and it was verified that they fluctuate randomly about constant mean values.

3.2. Pure compounds

The calculated density for the 10-repeat unit PVOH was 1.113 (± 0.014) g/cm³. This is approximately 12% lower than the reported density for amorphous PVOH of 1.26 g/cm³ [1] (isotactic PVOH, as used in the molecular

dynamics, has lower crystallinity than the syndiotactic and atactic forms [17] and thus calculated densities are compared to data for amorphous PVOH). When extrapolating to infinite repeat units from five sets of data each for 5, 7 and 10 repeat units the density is estimated as 1.227 g/cm³, which is only 2.6% lower than the reported value. The calculated Hildebrand solubility parameter for PVOH was 22.8 MPa^{0.5}, which is somewhat lower than reported experimental values [18] of 25–27 MPa^{0.5}. This is likely to be related to the lower density values. When density was fixed at 1.26 g/cm³, the calculated Hildebrand solubility parameter was 27.1 MPa^{0.5}, which is quite close to experimental values and compares well with the value of 27.0 MPa^{0.5} calculated using similar methods [10].

The calculated density for the 10-repeat unit PMVE-MA was 1.315 (± 0.023) g/cm³, which is about 5% lower than the experimental density of 1.378 (± 0.015) g/cm³ (determined from the film casting experiments). The calculated Hildebrand solubility parameter for PMVE-MA was 22.9 MPa^{0.5}. The estimated Hildebrand solubility parameter using the Hoftyzer–Van Krevelen group contribution method [11] is 21.7–22.6 MPa^{0.5}. Using the Bicerano connectivity indices method (Synthia module of the materials studio[®] suite of software [14]) it is estimated at 24.5–24.8 MPa^{0.5}. When density was fixed at 1.378 g/cm³, the calculated Hildebrand solubility parameter was 23.7 MPa^{0.5}. The solubility range determined using ASTM D3132-84 (1996) was 23–27 MPa^{0.5}, with the estimated solubility parameter from this method being 25.5 (± 2.5) MPa^{0.5}. Thus the calculated solubility parameter value falls within the solubility range determined experimentally.

3.3. Blend results—density, energy of mixing and Flory–Huggins interaction parameter

Fig. 3 compares the predicted densities to a simple linear volumetric mixing rule for the blends (which can be very simply derived from $\rho = m/V$, where ρ is density, m is the mass and V is the volume):

$$\rho_{\text{blend}} = \phi_A \rho_A + (1 - \phi_A) \rho_B \quad (1)$$

where ϕ_A is the volume fraction of polymer A.

There is a positive deviation from the linear mixing rule at 0.5–0.9 mass fraction PMVE-MA. This is consistent with the conventional model of an interpolymer complex—i.e. a

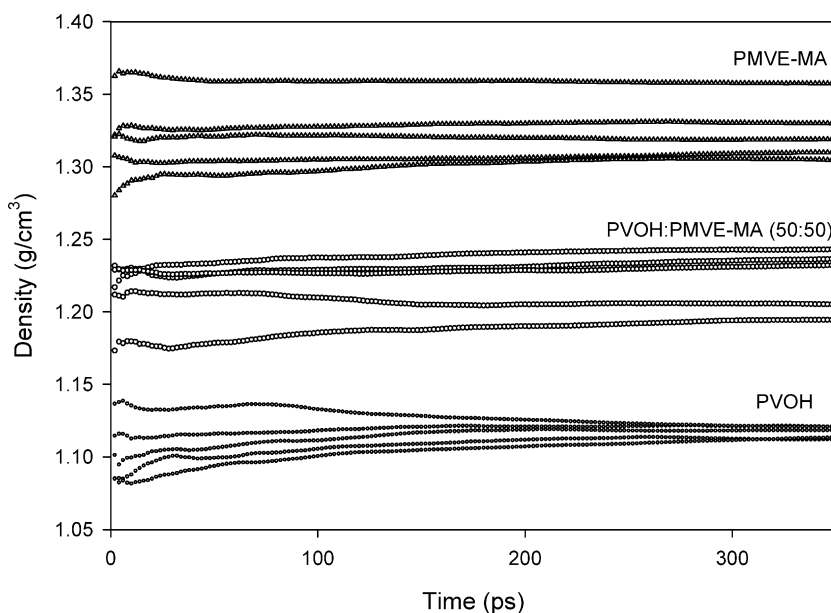


Fig. 2. Density of a selected number of runs (11–15) as a function of time.

denser packing of the two polymers resulting from the interpolymer interactions.

The solubility parameter, as defined by Hildebrand [19] is calculated using:

$$\delta = \sqrt{\frac{E_{\text{coh}}}{V}} \quad (2)$$

where E_{coh}/V is the cohesive energy density and

$$\frac{E_{\text{coh}}}{V} = \frac{\Delta H - RT}{V_M} \quad (3)$$

where ΔH is the heat of vaporization, R is the ideal gas constant, T the temperature and V_M is the molar volume; the cohesive energy is defined as the increase in energy per mole of a material if all intermolecular forces are eliminated.

The energy of mixing can be predicted from calculated cohesive energy densities (CED's) as follows [20]:

$$\frac{\Delta E_{\text{mix}}}{V} = \phi_A \left(\frac{E_{\text{coh}}}{V} \right)_A + \phi_B \left(\frac{E_{\text{coh}}}{V} \right)_B - \left(\frac{E_{\text{coh}}}{V} \right)_{\text{blend}} \quad (4)$$

where E_{coh}/V is the cohesive energy density.

According to the Flory–Huggins theory, the free energy of mixing per mole of lattice sites for a mixture of polymer A and polymer B is [20]:

$$\frac{\Delta \bar{G}_{\text{mix}}}{RT} = \left(\frac{\phi_A}{N_A} \right) \ln \phi_A + \left(\frac{\phi_B}{N_B} \right) \ln \phi_B + \chi \phi_A \phi_B \quad (5)$$

where N_A is the number of segments in polymer A and χ is the Flory–Huggins interaction parameter.

For favorable interaction between the blend components, one would expect negative χ -parameter values. The interaction parameters were estimated using [10]:

$$\chi = \frac{\Delta E_{\text{mix}}}{RT} V_{\text{mon}} \quad (6)$$

where V_{mon} is the monomer volume. This was arbitrarily taken as the molar volume of the smallest monomer in the blend (in this case vinyl alcohol or ethenol, with $M = 44.05$ g/mol). The molar volume of ethenol was estimated as $43 \text{ cm}^3/\text{mol}$ using a group contribution method [18].

It can be seen from Fig. 4 that the χ -parameters are negative for all blend compositions, with a minimum around 0.6–0.7 mass fraction PMVE-MA. The values have quite large standard deviations (similarly to [10]), possibly due to some of the cells being stuck in local energy minima instead of the global minimum. This possibility is also indicated by the variation obtained for equilibrium density (Fig. 2), which would translate into larger standard deviations for cohesive energy densities and consequently chi-parameters.

3.4. Blend results—solution viscosities

Fig. 5 shows the viscosity of blends of solutions of PVOH and PMVE-MA in different pH environments. For blends with unadjusted pH, there is a very clear optimum blend ratio for interpolymer complexation at around 10–14% PMVE-MA. Increase in PMVE-MA content at constant total polymer concentration led to a decrease in solution pH (data not shown), due to the dissociation of the carboxylic acid groups. Decrease in pH through addition of HCl leads to a shift in optimum blend ratio towards higher PMVE-MA content. With high levels of acid addition (dissolving the polymers in a 1 M HCl solution—starting pH of approximately 1), the optimum blend ratio is now around 0.7 mass fraction PMVE-MA. Decreasing pH also reduces absolute viscosities and broadens the optimum blend ratio peak.

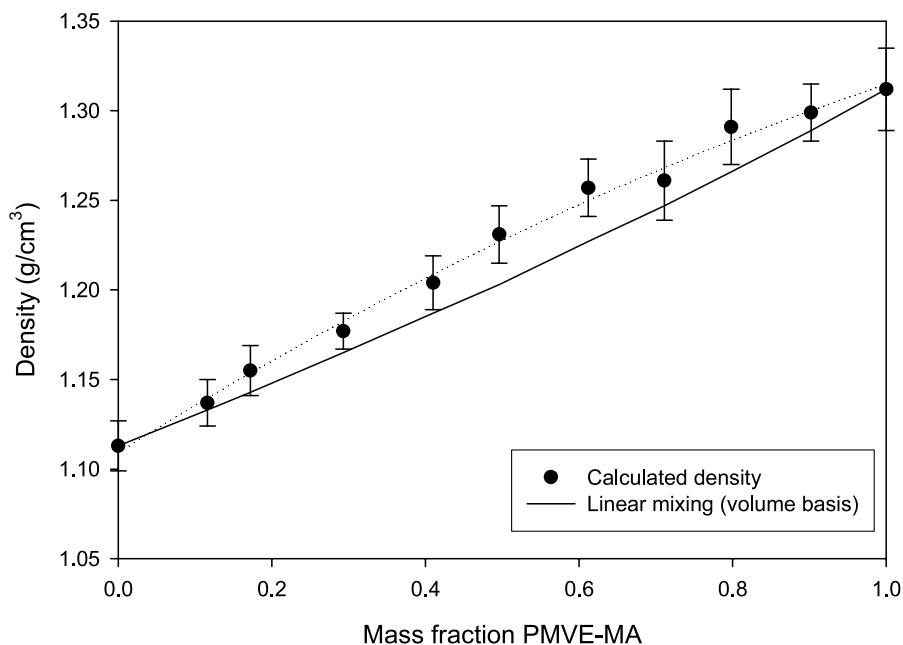


Fig. 3. Calculated density as a function of PMVE-MA mass fraction.

The cohesive energy densities display a positive deviation from linear mixing, and the optimum blend ratio from both the cohesive energy density and χ -parameter results corresponds well with that obtained from viscosity results at low pH, with the optimum blend ratio in the region of 0.7 mass fraction PMVE-MA (Fig. 6).

3.5. Radial distribution functions

A number of different combinations of intra- and intermolecular hydrogen bonding are possible. Table 2

lists the possible hydrogen-bonding interactions between oxygen and hydrogen atoms for PVOH and PMVE-MA, using the carbon atom numbering scheme in Fig. 7. The numbering scheme is explained by way of a number of examples: O1 corresponds to the oxygen bonded to carbon 1, while O8=C8 corresponds to the oxygen double-bonded to carbon 8, and O8–C8 is the oxygen with a single bond to carbon 8.

Fig. 8 shows a typical result for the radial distribution function—in this case for a 3:7 blend of PVOH:PMVE-MA and looking specifically at the interatomic distances

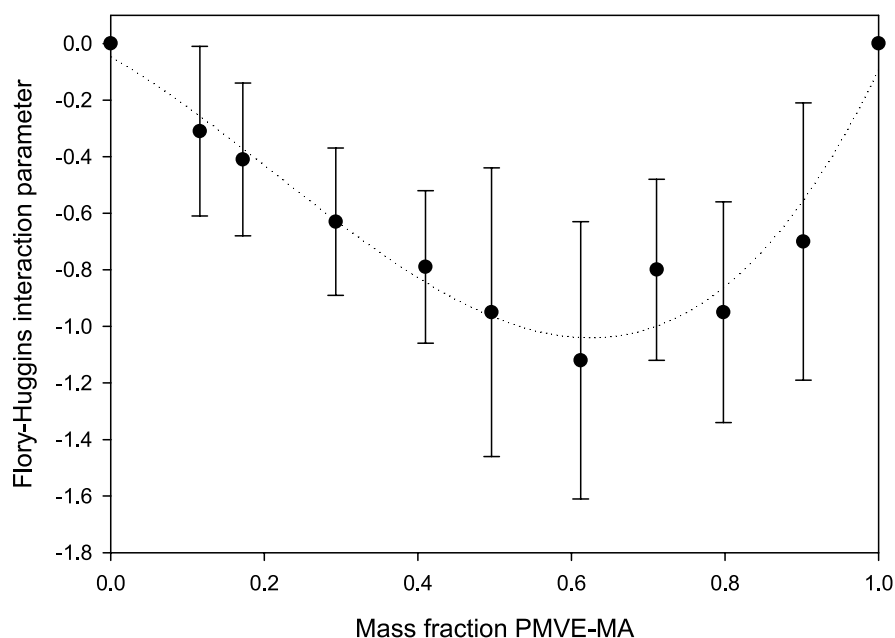


Fig. 4. The calculated Flory–Huggins interaction (χ) parameter as function of PMVE-MA mass fraction.

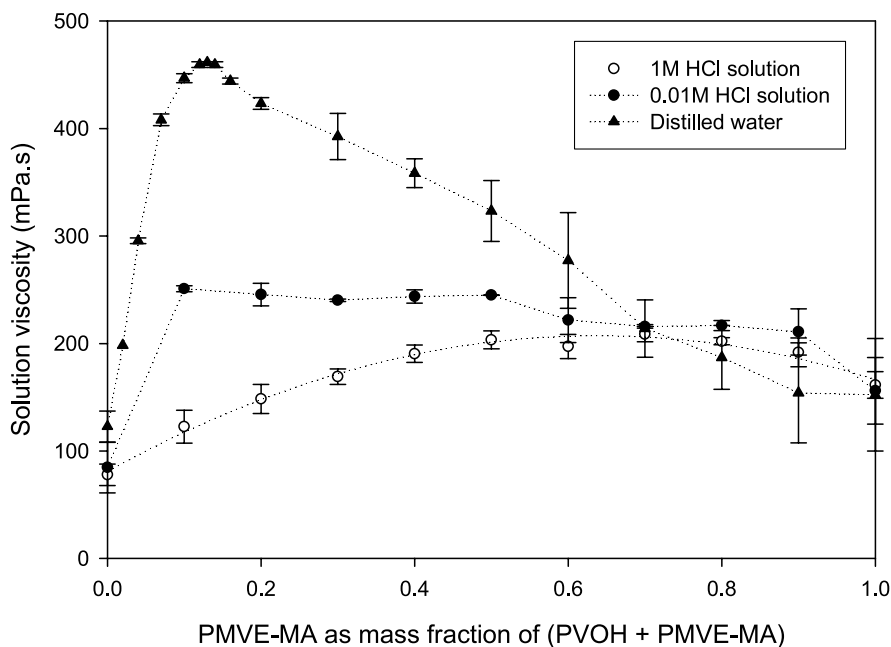


Fig. 5. Viscosity of PVOH:PMVE-MA blends at different pH-levels.

between the carbonyl oxygen of PMVE-MA and hydrogen atoms bonded to oxygen (interactions no. 3 and 7 from Table 2). Two major peaks are evident: one at an interatomic distance of 1.75 Å and the other at an interatomic distance of 2.35 Å. The peak at 2.35 Å is completely intramolecular and is due to the hydrogen contained on the same carboxylic acid group as the carbonyl oxygen. The peak at 1.75 Å is mostly due to intermolecular interactions—i.e. hydrogen bonds.

Table 3 contains calculated ratios of peak heights (intermolecular:intramolecular) of the radial distribution function at an interatomic distance of 1.65–1.75 Å. Looking at the hydrogen-bonding interactions number 4 and 8, there is a shift towards higher intermolecular hydrogen bonding for the 3:7 blend of PVOH:PMVE-MA compared to the pure PMVE-MA (inter/intra ratio changes from 0.74 to 0.85), indicating that the hydrogen atoms on the carboxylic acid groups of PMVE-MA form hydrogen bonds with the oxygen atoms on the alcohol groups of the PVOH. The decrease in total peak height seems to indicate reduced strength/occurrence of this interaction. This is possibly due to a rearrangement in the three-dimensional conformations of the chains due to other stronger interactions (see below).

The hydrogen-bonding interactions no. 1 and 5 indicate a clear shift towards intermolecular interaction for the blend when compared with PVOH on its own (inter/intra ratio changes from 0.26 to 0.70). This clearly indicates that the alcohol groups of the PVOH prefer to form hydrogen bonds with PMVE-MA rather than with itself. This is also indicated by the increase in total peak height, indicating increased strength/occurrence of this interaction.

4. Discussion

The polymer blend investigated is miscible in all ratios and has favorable interactions. Thus, we did not observe linear cohesive energy densities (as in e.g. [10]) as a function of volume fraction for blends of the two polymers. Rather, cohesive energy densities showed a positive deviation from linear mixing for all blend compositions, indicating favorable interaction.

Table 2
Possible hydrogen bonding interactions for PVOH:PMVE-MA blends

Interaction no.	Type	Interacting groups ^a
1	Intra- and intermolecular PVOH	H1...O1
2	Intra- and intermolecular PMVE-MA	H9...O8=C8 H8...O9=C9
3	Intra- and intermolecular PMVE-MA	H8...O8=C8 H9...O8=C8 H8...O9=C9 H9...O9=C9
4	Intra- and intermolecular PMVE-MA	H8...O4 H9...O4
5	Interpolymer complex	H8...O1 H9...O1
6	Interpolymer complex	H1...O8=C8 H1...O9=C9
7	Interpolymer complex	H1...O8=C8 H1...O9=C9
8	Interpolymer complex	H1...O4

^a Note that for each set of possible intra- and intermolecular interactions, there is a corresponding set of interpolymer complex interactions between similar groups (interactions 1 and 5; 2 and 6; 3 and 7; 4 and 8).

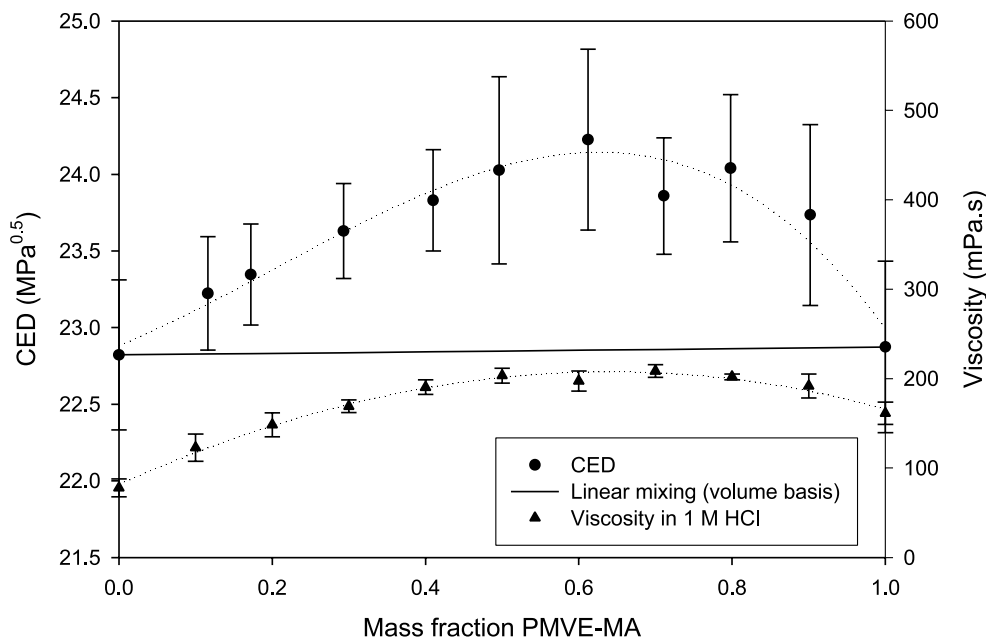


Fig. 6. Comparison of cohesive energy densities (calculated) and experimental viscosities at low pH.

The experimental systems and the molecular models differ in one major aspect: the model polymer cells consist of polymer chains in a ‘dry’ environment, whilst the experimental viscosity results were obtained in aqueous solution. At this stage we do not know exactly what the influence of the presence of water is on interpolymer complex formation between PVOH and PMVE-MA. However, based on the results from this study, it seems that this influence, at least in terms of optimum ratio of interaction, is small. Inclusion of water molecules in the models would increase the computational cost very significantly.

The calculated densities and cohesive energy density values were lower than experimental values, probably due to the relatively short chain lengths (10 repeat units for each oligomer) used in the modelling. Indeed, when density values were fixed at experimental density values, CED values were close to experimental values. The short chain lengths were chosen for two reasons: (1) to keep cell size/computing time at a manageable level (while maintaining a relatively realistic system—i.e. one long chain of each polymer would be a less realistic option than a few

shorter chains of each); and (2) to ensure sufficient mobility of chains to allow chain movement to form interpolymer complex interactions within the modelling time period.

The positive deviation of the calculated densities from the linear mixing rule seems to support the conventional model of an interpolymer complex as that of a denser network compared to the individual polymers due to the interpolymer interactions (a similar phenomenon was observed for hydrogen-bonded poly(methacrylic acid):poly(ethylene oxide) complex membranes, where higher contraction levels were observed for the complex membrane compared to the individual polymer membranes [21]).

The χ -parameter results also predict favorable interactions, with a minimum value (i.e. maximum interaction) around 0.6–0.7 mass fraction PMVE-MA, which correlates well with the experimental optimum of around 0.7 mass fraction PMVE-MA at low pH of approximately 1. Comparison of simulation results with viscosity results at low pH is justified because the carboxylic acid groups in the simulation cells are not dissociated (ionized). At pH below pK_a (negative logarithm of acid dissociation constant) of maleic acid (first and second dissociation constants at 25 °C are $pK_{a1}=1.91$ and $pK_{a2}=6.33$, respectively [22]), ionization of the carboxylic acid groups in the PMVE-MA is greatly reduced.

The experimental viscosity results at different pH indicate a large influence of pH on the optimum blend ratio between the two polymers. With decrease in pH (and thus decreasing degree of ionization of the carboxylic acid groups of the PMVE-MA), the optimum blend ratio shifts towards higher PMVE-MA content. This is possibly because of increased intra- and intermolecular hydrogen-bonding

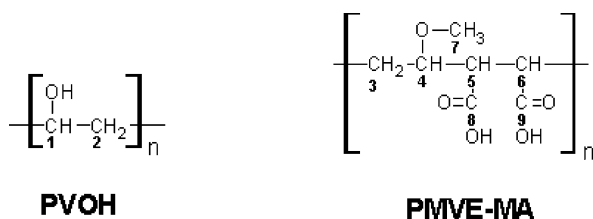


Fig. 7. Numbering scheme for carbon atoms in PVOH and PMVE-MA.

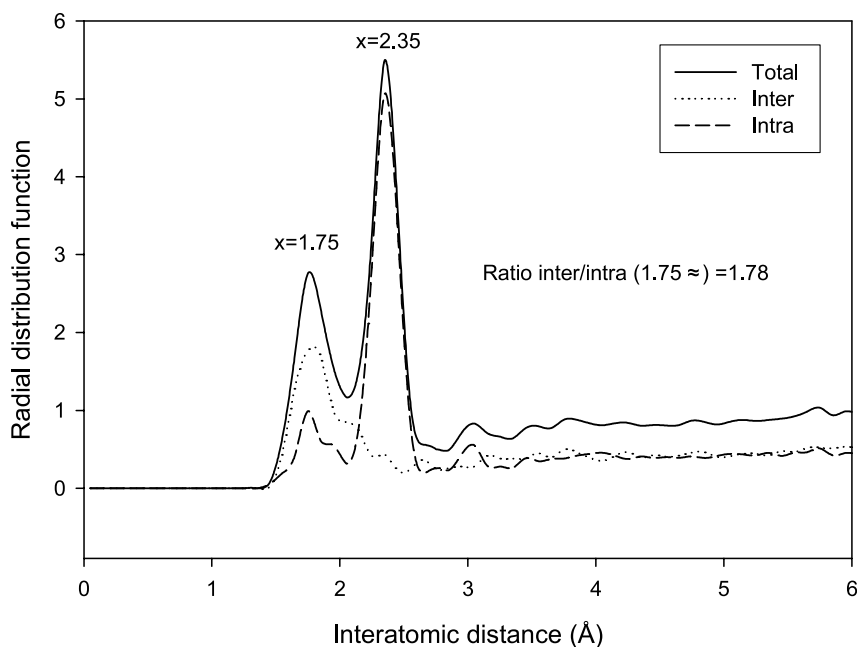


Fig. 8. Calculated radial distribution function for hydrogen bonding interactions no. 3 and 7 in an equilibrated 3:7 blend of PVOH:PMVE-MA.

within PMVE-MA at lower pH [21], thus leaving fewer groups available for intermolecular hydrogen-bonding with PVOH. Also, intramolecular repulsion due to negatively charged carboxylic groups is reduced with reduced ionization, allowing for more intra- and intermolecular hydrogen bonding within PMVE-MA.

The reduction in viscosity and broadening of the peak with decrease in viscosity can be explained by the same mechanism: with higher intramolecular hydrogen-bonding within PMVE-MA, interpolymer interaction is reduced, leading to a reduction in viscosity. The broadening of the peak is probably due to a larger number of possible hydrogen-bonding interactions that can occur at similar energy levels.

Because of the relatively large standard deviations for the χ -parameters a Student's *t*-test was performed for each value to determine the probability that these values are less than zero. The results indicated >99% probability (i.e. almost certainly) of not being zero for all blend values, and a probability of >99.99% of not being zero for values in the range 0.6–0.8.

The radial distribution function analysis indicates the formation of an interpolymer complex in the molecular

dynamics model, as increased intermolecular interactions (specifically hydrogen bonds) were observed for blends compared to the pure polymers.

5. Conclusions

Based on the above results, molecular dynamics seem to have potential for application in predicting polymer blend ratios for optimum interaction, especially where it proves difficult to determine the optimum ratios using conventional methods such as solution viscosity measurements (e.g. for designing new polymers with specific interaction ratios).

Further work is required to model the predicted optimum blend ratios in the presence of water, to determine whether molecular dynamics can provide realistic results for (partially) dissociated polymer complex systems.

Acknowledgements

Thanks are due to Michael Mkhize, Bram Dekkers and

Table 3

Ratios of peak heights (intermolecular:intramolecular) of radial distribution function at interatomic distance of 1.65–1.75 Å

Interaction no. (from Table 2)	System	Ratio of peak heights at 1.65–1.75 Å (inter:intra)	Total peak height
4 and 8	PMVE-MA	0.74	1.80
	3:7 PVOH:PMVE-MA	0.85	1.35
1 and 5	PVOH	0.26	4.16
	3:7 PVOH:PMVE-MA	0.70	6.74

Karl van Niekerk for some of the experimental viscosity data.

References

- [1] Brandrup J, Immergut EH, Grulke EA, editors. Polymer handbook. 4th ed. USA: Wiley; 1999.
- [2] Demetrakakis P. Barrier coatings help bottlers overcome shelf-life obstacles. Food Drug Packaging 2003 [http://www.findarticles.com/p/articles/mi_m0UQX/is_3_67/ai_99746654].
- [3] Truter P-A, Kruger AJ. Barrier technology. PCT Patent application PCT/IB 2004/001035; 2004.
- [4] Lowman AM, Peppas NA. Polymer 2000;41:73–80.
- [5] Bekturov EA, Bimendina LA. Adv Polym Sci 1981;41:99–147.
- [6] Quirke N. Industrial applications of molecular simulation ('Molecular simulation' S.). Switzerland: Gordon and B; 1989.
- [7] Goodman JM. Chemical applications of molecular modelling. UK: RSC; 1998.
- [8] Trohalaki S, Kloczkowski A, Mark JE, Rigby D, Roe RJ. Computer simulation of polymers. USA: Prentice-Hall; 1991.
- [9] Hofmann D, Fritz L, Ulbrich J, Schepers C, Bohning M. Macromol Theory Simul 2000;9:293.
- [10] Spyriouni T, Vergelati C. Macromolecules 2001;34:5306.
- [11] Van Krevelen DW. Properties of polymers. 3rd ed. Amsterdam: Elsevier Science; 1990 (chapters 6 and 7).
- [12] Allen MP, Tildesley DJ. Computer simulation of liquids. Oxford: Oxford University Press; 1987.
- [13] Leach AR. Molecular modelling, principles and applications. UK: Pearson Education Limited; 1996.
- [14] Accelrys Inc. San Diego; 2004.
- [15] Theodorou DN, Suter UW. Macromolecules 1985;18:1467.
- [16] Meirovitch HJ. J Chem Phys 1983;79:502.
- [17] Assender HE, Windle AH. Polymer 1998;39(18):4303–12.
- [18] Barton AFM. CRC handbook of solubility parameters and other cohesion parameters. 2nd ed. USA: CRC Press; 1991.
- [19] Hildebrand JH. Solubility. J Am Chem Soc 1916;38:1452.
- [20] Case FH, Honeycutt JD. Trends Polym Sci 1994;2(8):259–66.
- [21] Tsuchida E, Abe K. Adv Polym Sci 1982;45:1–119.
- [22] Martel AE, Smith RM. Critical stability constants. New York: Plenum Press; 1976.